Dye Adsorption on Layered Graphite Oxide

Philip Bradder, Sie King Ling, Shaobin Wang,* and Shaomin Liu

Department of Chemical Engineering, Curtin University of Technology, G.P.O. Box U1987, Perth, WA 6845, Australia

Graphite oxide (GO) was prepared by a modified Hummers−Offeman method and was tested as an adsorbent for the removal of dyes in aqueous solution. The structure of GO was characterized by N_2 adsorption, X-ray diffraction (XRD), and Fourier transform infrared (FT-IR) spectroscopy. It is found that GO does not show a significant change in surface area, but the layered graphene structure was expanded, and several surface oxygen functional groups were formed, which play a significant role in adsorption. The amount of the dyes, methylene blue and malachite green, adsorbed on the GO was much higher than that on graphite, and the adsorption capacity based on the Langmuir isotherm is (351 and 248) $mg \cdot g^{-1}$, respectively, much higher than activated carbon. The adsorption mechanism was proposed as electrostatic attraction.

Introduction

Recently, graphite oxide (GO) has generated a strong interest because of its intercalation property and as a precursor for graphene preparation. In general, GO is an oxygen-rich carbonaceous material, produced by the strong oxidation of graphite using $KMnO_4$ and H_2SO_4 or $HClO_4$. GO has various oxygen groups including epoxide, hydroxyl, carbonyl, and carboxyl groups. These oxygen functionalities render the GO as hydrophilic, and water molecules can readily intercalate into the interlayer galleries. Recently, many investigations have been reported on the preparation of intercalated GO[1−6] as nanocomposites. GO can also be used for other applications such as sensors and catalysts.[7] In fact, GO has a layered structure and various functional groups; it can also be used as an adsorbent. However, few investigations have been reported in this area recently. Seredych and Bandosz[7] investigated the removal of ammonia in gas by GO via its intercalation and reactive adsorption. They believed that the acid−base interactions with surface functional groups located at the edges of the carbon layers play a role in the mechanism of the removal process due to the basic property of ammonia. Matsuo et al.[8] also reported the removal of formaldehyde from the gas phase by silylated GO-containing amino groups. They found that the amount of formaldehyde adsorbed on this adsorbent was much higher than that on activated carbon, even when water molecules are preadsorbed. It was thus deduced that GO will also be good in adsorption of other compounds in water due to its hydrophilic/hydrophobic property change. However, few investigations have been reported on GO as an adsorbent for removal of chemical compounds from the aqueous phase. Our previous investigation has shown that GO could be used for the adsorption of humic acid.[9]

Wastewater discharged from the textile, printing, and tanning industries contains many dye stuffs, which can produce several effects on human beings, animals, and the environment. Recently, adsorption using activated carbon has been shown to be a simple and cost-effective method for the removal of contaminants in water.[10−12] However, the production of activated carbon and regeneration are expensive. In addition, activated carbon sometimes shows a low adsorption of ions. In this paper, we report an investigation of GO application in aqueous phase adsorption for dye removal.

* Corresponding author. E-mail: shaobin.wang@curtin.edu.au.

Materials and Methods

Synthesis of GO. For the preparation of GO, a natural graphite from Fluka was used. GO was prepared by a modified Hummers−Offeman method, and a detailed procedure can be found in the literature.[13] Typically, 50 g of H_2SO_4 (98 %) and 2 g of graphite were placed in a reactor cooled to 0 °C using iced water. After mixing the suspension for 30 min, 0.3 g of $KMnO_4$ was added in small portions to keep the temperature in the reactor not more than 10 °C. Thirty minutes later, 6 g of $KMnO_4$ was further added to the suspension gradually. After the $KMnO_4$ feeding was finished, the reactor was heated to about 35 °C and kept at this temperature for an additional 30 min. As the reaction progressed, the suspension became pasty and brownish in color. At the end of this 30 min period, 90 mL of water was slowly stirred into the paste to prevent violent effervescence, causing an increase in temperature from (90 to 95) °C. The diluted suspension, now brown in color, was maintained at this temperature for 15 min. The suspension was then further treated with a mixture of 7 mL of hydrogen peroxide (30 %) and 53 mL of water to reduce the residual permanganate and MnO_2 to soluble $MnSO_4$. The suspension was filtered and washed with distilled water three times, and the solids were collected by filtration and dried at 45 °C.

Characterization of GO. The surface area, total pore volume, and pore size distribution of all samples were determined by N_2 adsorption at −196 °C using Autosorb (Quantachrome Corp.). All samples were degassed at 200 °C for 4 h, prior to the adsorption experiments. The Brunauer−Emmett−Teller (BET) surface area and pore volume were obtained by applying the BET equation and $p/p_0 = 0.95$ to the adsorption data, respectively. The pore size distribution was obtained by the Barrett−Joyner−Halenda (BJH) method.

X-ray diffraction (XRD) patterns of all samples were obtained with an automated Siemens D500 Bragg−Brentano instrument using Cu Kα radiation at 40 kV and 40 mA over the range (2θ) of 10° to 90°, with a scanning speed at 2° per minute.

Fourier transfer infrared (FT-IR) spectra were collected on a Nicolet 6700 with a resolution of 4 cm^{-1} by using the attenuated

10.1021/je101049g
Published on Web 12/20/2010

Table 1. Physicochemical Properties of Graphite and GO

materials	S_{BET} / $m^2 \cdot g^{-1}$	V / $cm^3 \cdot g^{-1}$	average pore size / nm	slurry pH
graphite	16.6	0.092	18.8	6.9
GO	28.5	0.088	19.5	4.3

total reflectance (ATR) technique. The spectrum was scanned from (400 to 4000) cm^{-1}.

The pH of the samples was measured as follows: 0.01 g of graphite and GO samples were mixed with 10 mL of distilled water and shaken for 24 h at 30 °C. After filtration, the pH of solution was determined by a pH meter (Radiometer PHM250 ion analyzer).

Adsorption Test. For dye adsorption, two cationic dyes, methylene blue (MB) and malachite green (MG), were obtained from Aldrich Chemicals. For the adsorption test on graphite, 100 mg of solid was put into 80 mL of dye solution, which was then subjected to 600 rpm stirring at 25°. At a preset time interval, a dye sample was withdrawn and placed in a centrifuge for separation at 3750 rpm for 2 min. Then, the supernatant liquid was drawn off and analyzed using a UV−vis spectrophotometer at wavelengths of (663 and 617) nm for MB and MG, respectively. For the GO adsorption test, a similar procedure was taken; however, the amount of GO and solution volume were different. In each run, 10 mg of GO was put into 500 mL of a given concentration of MB or MG solution stirred at 600 rpm.

Results and Discussion

Table 1 presents the physicochemical properties of graphite and GO. N_2 adsorption shows that graphite has a BET surface area and pore volume of 17 $m^2 \cdot g^{-1}$ and 0.092 $cm^3 \cdot g^{-1}$, respectively. The pore volume was calculated at a relative pressure of 0.96. After oxidation, GO has a surface area of 28 $m^2 \cdot g^{-1}$ and pore volume of 0.088 $cm^3 \cdot g^{-1}$. GO also has a high average pore size, suggesting the expansion of the graphene layer. Slurry pH values of graphite and GO also indicate that GO exhibits strong acidity while graphite is almost neutral.

Figure 1 shows XRD profiles of graphite and GO. XRD analysis indicates a very intense and narrow peak at $2\theta = 26.5°$ corresponding to the (002) planes of graphene layers occurring in graphite. Three other peaks at $2\theta = 42.5°$, 44.6°, and 54° can also be observed, corresponding to (100), (101), and (004). For GO, a strong peak at $2\theta = 10.4°$ occurs, which is the structure expansion as oxygen-containing groups incorporate between the carbon sheets during the course of strong oxidation. In addition, two weak peaks at $2\theta = 22.0°$ and 42.5° also occur. These peaks are similar to typical GO XRD patterns reported previously.[4,13]

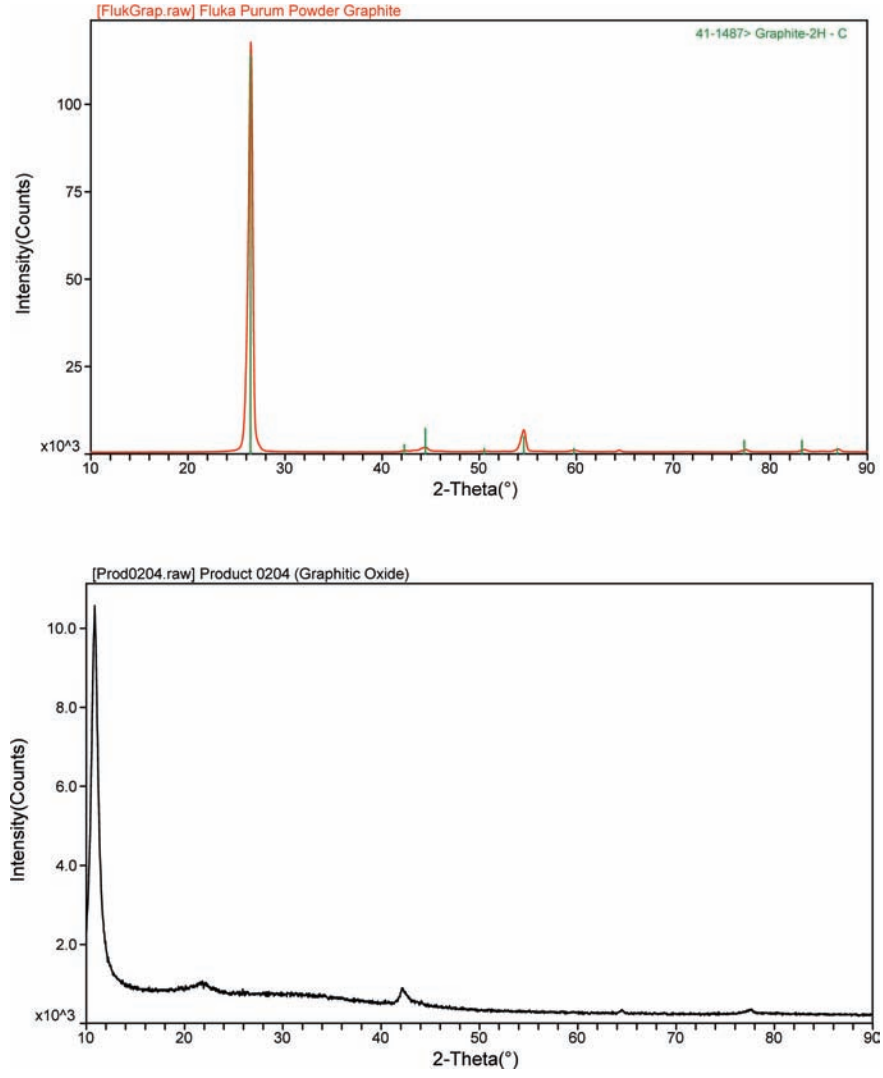

Figure 1. XRD profiles of graphite and GO.

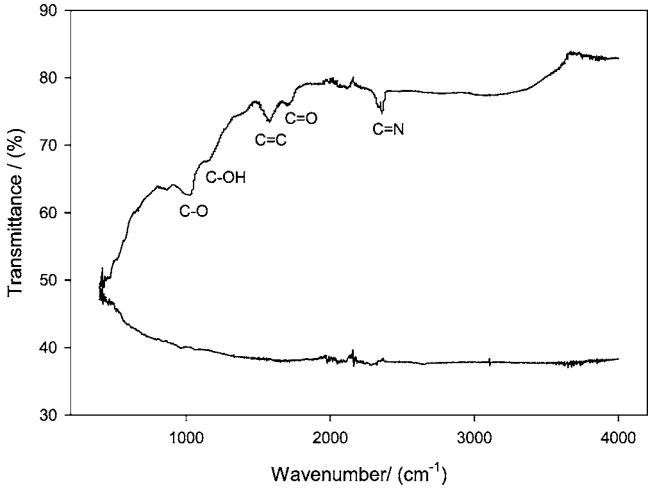

Figure 2. FT-IR spectra of graphite and GO.

Figure 2 illustrates the FT-IR spectra of graphite and GO. The results show that the graphite exhibits no functional groups on the surface, while the GO presents several functional groups. The broad spectra between (3000 and 3600) cm^{-1} is due to the stretching vibrations of structural OH groups. The band at 1706 cm^{-1} can be ascribed to the C═O stretching of COOH groups, and the band at 1577 cm^{-1} can be assigned to aromatic C═C vibration. The strong band at 1050 cm^{-1} is due to the vibration of C—O, and the weak band at 1200 cm^{-1} will be due to phenolic groups.

Figure 3 shows the dynamic adsorption of MB and MG on graphite and GO. As seen, MB and MG adsorption on graphite reaches equilibrium at around (40 to 60) min, which is due to the strong stirring rate and fast mass transfer. However, the equilibrium adsorption on graphite is quite low. The graphite exhibits MB and MG adsorption at (3 and 6) $mg \cdot g^{-1}$, respectively. Meanwhile, GO also presents a fast adsorption rate reaching equilibrium at 20 min. Compared with graphite, GO presents much higher adsorption at (220 and 180) $mg \cdot g^{-1}$, for MB and MG, respectively. As shown in Table 1, one can see that the textural structure of graphite and GO is similar. Thus, the higher adsorption of MB and MG on GO is not due to the surface physical properties such as surface area and pores but due to the surface chemistry.

The adsorption kinetics was modeled using the pseudosecond-order model, which is expressed in eq 1:

$$q_t = \frac{q_e^2 k_2 t}{1 + k_2 q_e t} \quad (1)$$

where q_e and q_t are the amounts of solute adsorbed ($mg \cdot g^{-1}$) at equilibrium and time t (min), respectively, and k_2 is the rate constant of the pseudosecond-order adsorption ($mg \cdot g^{-1} \cdot min^{-1}$). Figure 3 also shows the curve fit to the experimental data by the model, and the parameters obtained are presented in Table 2. The results indicate that dye adsorption on graphite and GO can be well-described by the pseudosecond-order kinetic model.

XRD shows the expansion of the layered structure of GO, and FT-IR also exhibits the presence of various oxygen functional groups such as epoxy, −OH, and −COOH. It is generally believed that −COOH groups exist at the edges of carbon layers and epoxy and hydroxyl groups are incorporated in the layers,[8] thus resulting in an acidic surface or negatively charged surface, which can be proved by the low slurry pH of

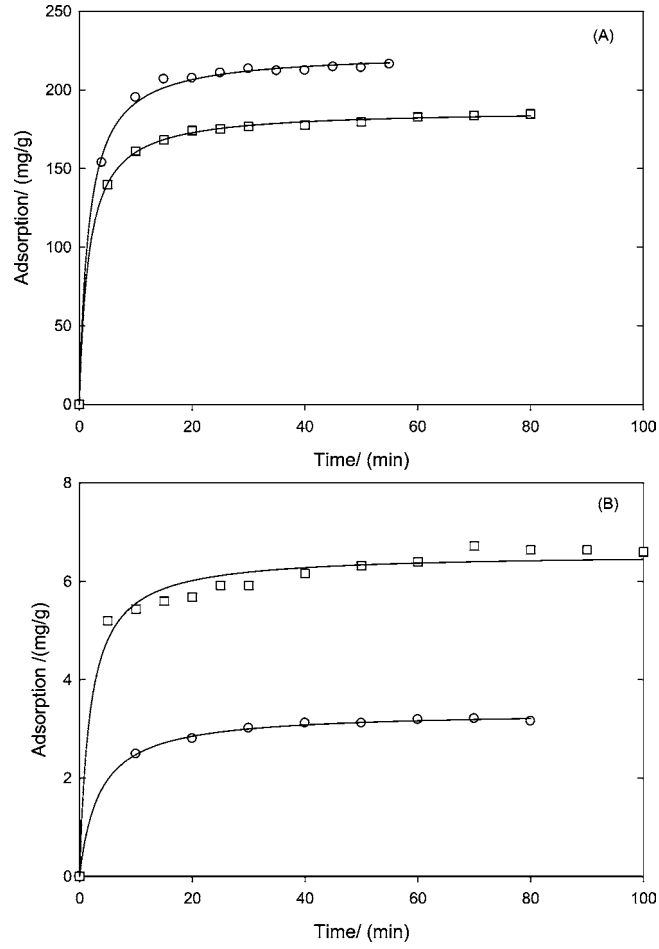

Figure 3. Comparison of MB and MG adsorption on graphite and GO. (A) GO; (B) graphite; ○, MB; □, MG; solid line, second-order kinetics.

Table 2. Parameters of Pseudosecond Order Kinetics for MB and MG Adsorption on Graphite and GO

	MB			MG		
	q_e	k_2		q_e	k_2	
adsorbate	$mg \cdot g^{-1}$	$g \cdot mg^{-1} \cdot min^{-1}$	R^2	$mg \cdot g^{-1}$	$g \cdot mg^{-1} \cdot min^{-1}$	R^2
graphite	3.3	0.085	0.999	6.6	0.083	0.982
GO	223.8	$2.66 \cdot 10^{-3}$	0.998	187.1	$3.19 \cdot 10^{-3}$	0.999

GO (Table 1). MB and MG are cationic dyes, which will exist as positively charged ions in aqueous solution. Therefore, the adsorption of MB and MG on GO can be attributed to electrostatic attraction. The mechanism is proposed as follows.

$$C{-}COO^- + CS^+(MB) \rightarrow C{-}COOCS \quad (2)$$

$$C{-}COO^- + CN^+(MG) \rightarrow C{-}COOCN \quad (3)$$

Figure 4 displays MB and MG adsorption isotherms on GO and two adsorption models, Langmuir (eq 4) and Freundlich (eq 5) isotherms, for experimental curve fitting.

$$q_e = \frac{K_L \cdot q_{max} \cdot C_e}{1 + K_L \cdot C_e} \quad (4)$$

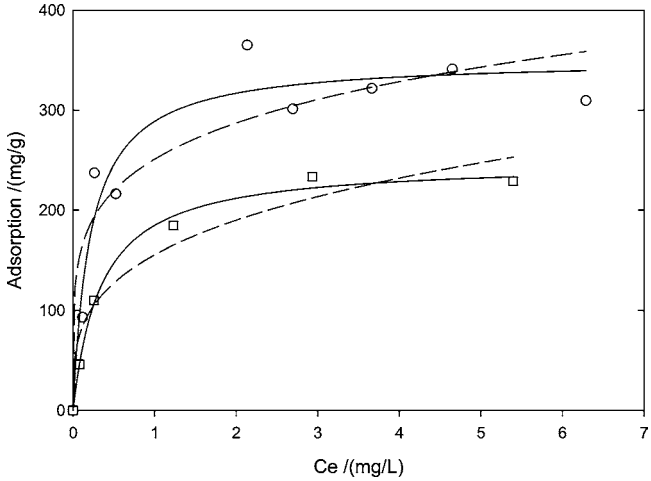

Figure 4. Adsorption isotherms of MB and MG on GO at 25 °C. ○, MB; □, MG; solid line, Langmuir isotherm; dotted line, Freundlich isotherm.

Table 3. Parameters of Adsorption Isotherms from Langmuir and Freundlich Models

	Langmuir isotherm			Freundlich isotherm		
	Q_{max}	K				
dye	mg·g^{-1}	L·mg^{-1}	R^2	K	1/n	R^2
MB	351.1	4.63	0.939	250.9	0.194	0.871
MG	248.1	2.92	0.995	155.4	0.289	0.952

$$q_e = K_F C_e^{1/n} \quad (5)$$

where K_L is the Langmuir adsorption constant (L·mg^{-1}) related to the energy of adsorption, q_{max} is adsorption capacity (mg·g^{-1}), C_e is the equilibrium liquid phase concentration (mg·L^{-1}), and q_e is the equilibrium adsorption (mg·g^{-1}). K_F is the Freundlich constant (L·mg^{-1}), and (1/n) is the heterogeneity factor. The curve fit and parameters from the models are presented in Figure 4 and Table 3, respectively.

As shown, MB and MG present strong adsorption on GO, and MB adsorption is higher than MG. For the two isothermal models, the experimental data are better fitted by the Langmuir isotherm, evidenced by the higher regression coefficient. On the basis of the Langmuir model, the maximum adsorption of MB and MG on GO is around (350 and 248) mg·g^{-1}, respectively. Our previous investigations on methylene blue adsorption on various adsorbents such as activated carbon,[14] unburned carbon from fly ash,[15] and zeolitic MCM-22[16] have given adsorption capacities as (189, 80, and 57) mg·g^{-1}, respectively. For MG, Gupta et al.[17] reported an adsorption capacity on a commercial activated carbon as 75.1 mg·g^{-1}. Malik et al.[18] also reported an adsorption capacity of the activated carbon prepared from groundnut shell waste at 222 mg·g^{-1}. Wang and Ariyanto[19] investigated MG adsorption on a natural zeolite and obtained an adsorption capacity of 19 mg·g^{-1}. Thus, it is clearly shown that GO has a much higher adsorption capacity than some of activated carbons and other adsorbents.

Conclusions

In this work, GO was synthesized and tested for dye adsorption. Characterization has shown that surface acidity and several oxygen functional groups play the major role in cationic dye adsorption. For MB and MG, the adsorption capacity is (350 and 248) mg·g^{-1}, respectively, higher than some activated carbons. The adsorption mechanism can be attributed to electrostatic attraction. Thus, GO will be a promising adsorbent for cationic ion removal in aqueous solution.

Literature Cited

(1) Matsuo, Y.; Tahara, K.; Sugie, Y. Synthesis of poly(ethylene oxide)-intercalated graphite oxide. *Carbon* **1996**, *34*, 672–674.
(2) Matsuo, Y.; Nishino, Y.; Fukutsuka, T.; Sugie, Y. Introduction of amino groups into the interlayer space of graphite oxide using 3-aminopropylethoxysilanes. *Carbon* **2007**, *45*, 1384–1390.
(3) Xu, J. Y.; Hu, Y. A.; Song, L.; Wang, Q. G.; Fan, W. C. Preparation and characterization of polyacrylamide-intercalated graphite oxide. *Mater. Res. Bull.* **2001**, *36*, 1833–1836.
(4) Bissessur, R.; Liu, P. K. Y.; Scully, S. F. Intercalation of polypyrrole into graphite oxide. *Synth. Met.* **2006**, *156*, 1023–1027.
(5) Chua, Y. H.; Yamagishi, M.; Wang, Z. M.; Kanoh, H.; Hirotsu, T. Adsorption characteristics of nanoporous carbon-silica composites synthesized from graphite oxide by a mechanochemical intercalation method. *J. Colloid Interface Sci.* **2007**, *312*, 186–192.
(6) Liu, P. G.; Gong, K. C. Synthesis of polyaniline-intercalated graphite oxide by an in situ oxidative polymerization reaction. *Carbon* **1999**, *37*, 706–707.
(7) Seredych, M.; Bandosz, T. J. Removal of ammonia by graphite oxide via its intercalation and reactive adsorption. *Carbon* **2007**, *45*, 2130–2132.
(8) Matsuo, Y.; Nishino, Y.; Fukutsuka, T.; Sugie, Y. Removal of formaldehyde from gas phase by silylated graphite oxide containing amino groups. *Carbon* **2008**, *46*, 1162–1163.
(9) Hartono, T.; Wang, S.; Ma, Q.; Zhu, Z. Layer structured graphite oxide as a novel adsorbent for humic acid removal from aqueous solution. *J. Colloid Interface Sci.* **2009**, *333*, 114–119.
(10) Ali, I.; Gupta, V. K. Advances in water treatment by adsorption technology. *Nature Protocols* **2007**, *1*, 2661–2667.
(11) Gupta, V. K.; Carrott, P. J. M.; Ribeiro Carrott, M. M. L. Suhas, Low cost adsorbents: Growing approach to wastewater treatment - A review. *Crit. Rev. Environ. Sci. Technol.* **2009**, *39*, 783–842.
(12) Gupta, V. K.; Suhas. Application of low cost adsorbents for dye removal - A review. *J. Environ. Manage.* **2009**, *90*, 2313–2342.
(13) Titelman, G. I.; Gelman, V.; Bron, S.; Khalfin, R. L.; Cohen, Y.; Bianco-Peled, H. Characteristics and microstructure of aqueous colloidal dispersions of graphite oxide. *Carbon* **2005**, *43*, 641–649.
(14) Wang, S. B.; Zhu, Z. H.; Coomes, A.; Haghseresht, F.; Lu, G. Q. The physical and surface chemical characteristics of activated carbons and the adsorption of methylene blue from wastewater. *J. Colloid Interface Sci.* **2005**, *284*, 440–446.
(15) Wang, S. B.; Li, L.; Wu, H. W.; Zhu, Z. H. Unburned carbon as a low-cost adsorbent for treatment of methylene blue-containing wastewater. *J. Colloid Interface Sci.* **2005**, *292*, 336–343.
(16) Wang, S. B.; Li, H.; Xu, L. Y. Application of zeolite MCM-22 for basic dye removal from wastewater. *J. Colloid Interface Sci.* **2006**, *295*, 71–78.
(17) Gupta, V. K.; Srivastava, S. K.; Mohan, D. Equilibrium uptake, sorption dynamics, process optimization, and column operations for the removal and recovery of malachite green from wastewater using activated carbon and activated slag. *Ind. Eng. Chem. Res.* **1997**, *36*, 2207–2218.
(18) Malik, R.; Ramteke, D. S.; Wate, S. R. Adsorption of malachite green on groundnut shell waste based powdered activated carbon. *Waste Manage.* **2007**, *27*, 1129–1138.
(19) Wang, S.; Ariyanto, E. Competitive adsorption of malachite green and Pb ions on natural zeolite. *J. Colloid Interface Sci.* **2007**, *314*, 25–31.

Received for review October 18, 2010. Accepted December 3, 2010.

JE101049G